

Competing Spin-Gap Phases in a Frustrated Quantum Spin System in Two Dimensions

Yoshihiro Takushima, Akihisa Koga, and Norio Kawakami

Department of Applied Physics, Osaka University, Suita, Osaka 565-0871

(Received October 24, 2018)

We investigate quantum phase transitions among the spin-gap phases and the magnetically ordered phases in a two-dimensional frustrated antiferromagnetic spin system, which interpolates several important models such as the orthogonal-dimer model as well as the model on the 1/5-depleted square lattice. By computing the ground state energy, the staggered susceptibility and the spin gap by means of the series expansion method, we determine the ground-state phase diagram and discuss the role of geometrical frustration. In particular, it is found that a RVB-type spin-gap phase proposed recently for the orthogonal-dimer system is adiabatically connected to the plaquette phase known for the 1/5-depleted square-lattice model.

KEYWORDS: frustration, quantum phase transition, series expansion, two dimensional spin system

§1. Introduction

Geometrical frustration plays an important role for the spin-gap formation in a certain class of antiferromagnetic quantum spin systems. Two typical spin-gap compounds found in two dimension (2D) are the transition metal oxides, $\text{SrCu}_2(\text{BO}_3)_2$ ¹⁾ and CaV_4O_9 .²⁾ In the former compound, the orthogonal-dimer structure of the Cu^{2+} spins stabilizes the dimer phase with the spin gap, which is properly described by the 2D Heisenberg model on the square lattice with diagonal interactions (Shastry-Sutherland model),³⁾ as claimed by Miyahara and Ueda.⁴⁾ For the model, it was pointed out that there should exist an intermediate phase between the dimer and the antiferromagnetic phases,⁵⁻⁷⁾ implying that strong frustration due to the competing interactions is quite important for understanding this model. On the other hand, the latter spin-gap compound CaV_4O_9 may be described by the 2D Heisenberg model on the 1/5-depleted square lattice⁸⁾ or the meta-plaquette model.^{9,10)} The spin-gap phase in this compound results from the plaquette-singlet formation, which is further stabilized by the frustration effect due to the next-nearest-neighbor interactions.

An interesting feature common to the above systems is that geometrical frustration due to the competing interactions plays an essential role to stabilize the disordered ground state. It is thus important to deal with these systems in a unified framework to clarify the role of frustration systematically. In particular, since a RVB-type spin-gap phase⁶⁾ proposed for the Shastry-Sutherland model may be caused by geometrical frustration, it is desired to further clarify the nature of this spin-gap phase. This is also important from the experimental point of view, because the compound $\text{SrCu}_2(\text{BO}_3)_2$ is expected to be located around the phase boundary between the dimer and RVB-type phases.

Motivated by the above hot topics, we study the com-

petition among the spin-gap phases as well as the magnetically ordered phases in a 2D frustrated quantum spin system on the square lattice with some diagonal couplings. The basic idea in this paper is the adiabatic continuation, which allows us to relate apparently different states which belong to the same phase at the fixed point. By using this model, we systematically describe quantum phase transitions for the orthogonal-dimer model and the Heisenberg model on the 1/5-depleted square lattice, where the ground-state phase diagram was already discussed in detail.^{4-7,11,12)} In particular, we show that a RVB-type spin-gap phase naturally emerges in the Shastry-Sutherland model, by observing the adiabatic evolution of the spin-gap state when the competing interactions are varied.

This paper is organized as follows. In §2, we introduce a 2D frustrated spin model, which allows us to treat the above spin-gap compounds systematically. After briefly summarizing the series expansion method in §3, we investigate the first- and second-order quantum phase transitions among the spin-gap phases and the magnetically ordered phases in §4. We there determine the phase diagram and clarify the role of geometrical frustration in this class of quantum spin systems. A brief summary is given in §5.

§2. Model Hamiltonian

We consider the Heisenberg model on the square lattice with some diagonal couplings, which is described by the Hamiltonian

$$H = J \sum_{\text{diagonal}} \mathbf{S}_i \cdot \mathbf{S}_j + J' \sum_{\text{square}} \mathbf{S}_i \cdot \mathbf{S}_j, \quad (2.1)$$

where \mathbf{S}_i is the $s = 1/2$ spin operator at the i -th site, and J , J'_1 and J'_2 represent the antiferromagnetic exchange couplings. By putting J on the orthogonal dimer bonds (dashed lines), we then distribute the other couplings J'_1 and J'_2 in two ways as shown in Figs. 1(a) and 1(b). In

the case (a), there is a diagonal bond J in each plaquette formed by the coupling J'_1 (bold line), while in the case (b) there is no diagonal bond in shaded plaquettes. What is interesting in this generalization is that we can discuss several different models in the same framework. Namely, both models of (a) and (b) are related to each other via the Shastry-Sutherland model with $J'_1 = J'_2$, and moreover they are reduced to the well-known models in the limiting case of $J'_2 = 0$: the orthogonal-dimer chain for (a) and the spin system with a windmill structure for (b). Note that the latter is topologically equivalent to the Heisenberg model on the 1/5-depleted square lattice for the compound CaV_4O_9 . Therefore, by using the above models we can systematically study how the geometrical frustration in the 2D model affects the generation of the spin gap. For later convenience, we introduce the ratios $\alpha = J'_1/J$ and $k = J'_2/J$.

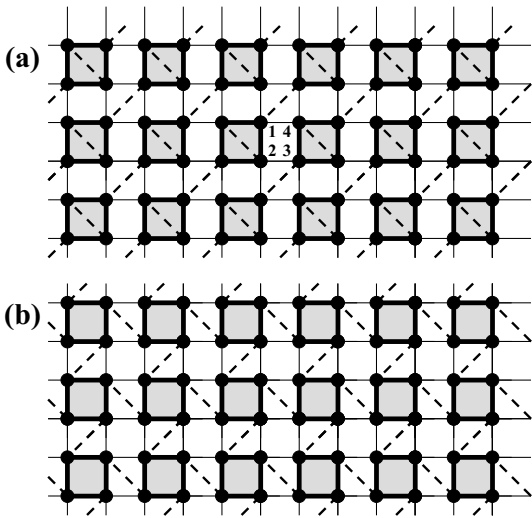


Fig. 1. Frustrated spin models on the square lattice with some diagonal bonds. The bold, thin and dashed lines represent the coupling constants J'_1 , J'_2 and J . The initial configuration of the isolated dimers (plaquettes) for the series expansion is indicated by the dashed lines (shaded squares).

§3. Series Expansion Method

In order to study quantum phase transitions, we make use of the series expansion method.¹³⁾ This method is powerful especially for quantum spin systems with frustration, where quantum Monte Carlo simulations may suffer from sign problems. In the present context, we wish to mention that this method was successfully applied to the meta-plaquette system,^{9,10)} the orthogonal dimer system,^{6,7,11,14)} etc. To determine the phase diagram, we consider two initial configurations in the series expansion. The first one is a plaquette-singlet configuration composed of the shaded squares in Figs. 1(a) and 1(b). In this case, we parameterize the antiferromagnetic couplings labeled by the bold, thin and dashed lines as $J'_1, J'_2 = \lambda k J'_1$ and $J = \lambda J'_1/\alpha$, where we have introduced an auxiliary series-expansion parameter λ in addition to the dimensionless couplings k and α . The original model we are interested in is recovered by setting

$\lambda = 1$. Note that a RVB-type spin-gap phase,⁶⁾ which has the spatially-extended disordered ground state, may be reached in this approach. The second one is a dimer configuration, by which we can describe the dimer phase. A convenient parameterization in the dimer expansion is $J(=1), J'_1 = \lambda\alpha$ and $J'_2 = \lambda k\alpha$. In this way, these two different approaches enable us to perform the series expansion starting from isolated dimer and plaquette singlets ($\lambda = 0$).

To carry out the series expansion explicitly, the original Hamiltonian eq.(2.1) is divided into two parts,

$$H = H_0 + \lambda H_1$$

$$= x \left[\sum \mathbf{S}_i \cdot \mathbf{S}_j + \lambda \sum \Gamma_{ij} \mathbf{S}_i \cdot \mathbf{S}_j \right], \quad (3.1)$$

where $x = J/J'_1$ and $\Gamma_{ij} = \alpha$ or $k\alpha$ (k or α^{-1}) for the dimer (plaquette) expansion. The first term H_0 is the unperturbed Hamiltonian which stabilizes the isolated dimer or plaquette singlets, whereas the perturbed Hamiltonian H_1 labeled by λ connects these isolated dimer or plaquette singlets, yielding a 2D frustrated spin system. We compute the staggered susceptibility χ_{AF} , the spin-triplet excitation energy $E(\mathbf{q})$, and the ground state energy E_g as a power series in λ . To estimate the susceptibility, we introduce the Zeeman term

$$H' = h \left[\sum_{i \in A} \mathbf{S}_i^z - \sum_{i \in B} \mathbf{S}_i^z \right], \quad (3.2)$$

where h is the staggered magnetic field and $A(B)$ denotes one of the two sublattices.

We determine the quantum phase transition point in three ways: (i) comparison of the ground state energy, (ii) divergence of the staggered susceptibility, (iii) vanishing point of the spin gap. The latter two schemes may be applied to the second-order phase transition, while the first one is more effective to study the first-order phase transition. In order to obtain the accurate phase boundary, we further use the Dlog Padé approximants¹⁵⁾ for the calculated results up to the finite order in λ . We also make use of the *biased* Padé approximants,¹⁵⁾ in which the critical exponents for our 2D quantum spin model are assumed to take those expected for the 3D classical Heisenberg model.¹⁶⁾ The phase-transition point, λ_c , is then determined by the formula $\chi_{AF} \sim (\lambda_c - \lambda)^{-\gamma}$ and $\Delta \sim (\lambda_c - \lambda)^\nu$ with the critical exponents $\gamma = 1.4$ and $\nu = 0.71$.¹⁷⁾

§4. Quantum Phase Transitions

We now discuss quantum phase transitions when the competing exchange couplings are varied. There are three parameters in the perturbation term, λ, α and k . We first study the model given by Fig. 1(a), which continuously connects the 2D Shastry-Sutherland model and the 1D orthogonal-dimer chain, and then move to the model (b), which includes the Heisenberg model on the 1/5 depleted square lattice.

4.1 Adiabatic evolution from the orthogonal-dimer chain

Let us start with the system shown in Fig. 1(a). Note that this spin system is reduced to the orthogonal-dimer chain for $k = 0$, which was already studied in detail: when the ratio α of the competing exchange couplings is varied, the first-order quantum phase transition between the spin-gap phases with the dimer and the plaquette structures occurs at $\alpha_{c1} = 0.81900$.^{11,18)} The merit to study this system is that we can check how the known spin-gap states in the chain system adiabatically evolve when the system approaches the 2D Shastry-Sutherland model.

We first discuss the effect of interchain coupling k on the first-order phase transition between two spin-gap phases by computing the ground state energy E_g . Note that the energy for the dimer phase is unchanged even on the introduction of k due to the orthogonal-dimer structure.³⁾ For the plaquette phase, by choosing the isolated plaquettes shown by shaded squares in Fig. 1(a) as an initial configuration, we compute the ground state energy E_g up to the sixth order in λ with α and k being fixed. By applying the first-order inhomogeneous differential method to the obtained series, we then estimate the ground state energy for the plaquette phase by setting $\lambda = 1$. The energy estimated for $k = 0.1, 0.5$ and 0.9 is shown in Fig. 2. It is seen that the introduction

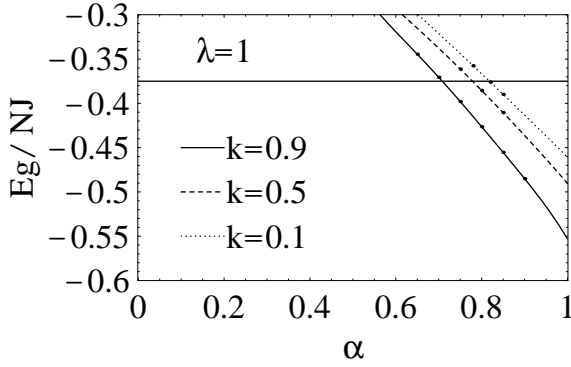


Fig. 2. Ground state energy per site as a function of $\alpha = J'_1/J$ (for $\lambda = 1$). The flat line ($E_g/JN = -3/8$) is the energy for the exact dimer state. The dotted, dashed and solid lines denote the energy at $\lambda = 1$ obtained by the plaquette expansion for $k = 0.1, 0.5$ and 0.9 , respectively.

of k prefers the plaquette phase, shifting the first-order transition point α_{c1} to the left in Fig. 2. From these analyses, we determine the phase boundary between the dimer phase and the plaquette phase in the 2D parameter space, which is shown in Fig. 3. We have checked that the present estimate of the critical point for $k = 0$ reproduces the above-mentioned value of α_{c1} fairly well. It is seen that the phase boundary is not so sensitive to k for small k , because the energy for the plaquette phase decreases quadratically in k .

It is to be noted that these two competing spin-gap phases are continuously connected to those in the Shastry-Sutherland model ($k = 1$), with the nature of the first-order transition being unchanged.⁶⁾ To check the va-

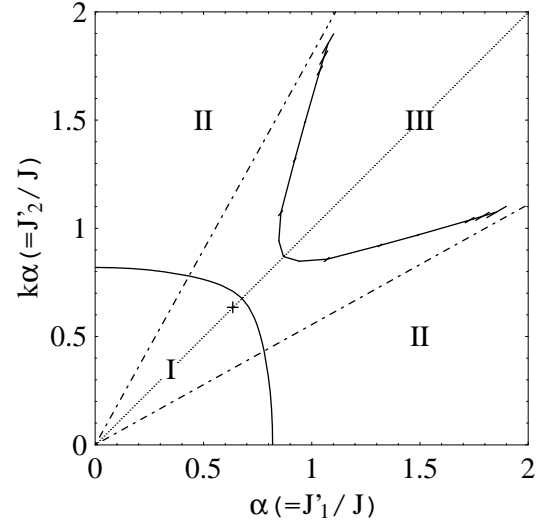


Fig. 3. Phase diagram for the 2D frustrated spin system shown in Fig. 1(a). The phases I, II and III represent the dimer, plaquette and magnetically ordered phases, respectively. The dotted line corresponds to the 2D Shastry-Sutherland model and the dot-dashed lines to the asymptotic phase boundary for large α . The cross indicates the parameters deduced for $\text{SrCu}_2(\text{BO}_3)_2$.¹⁹⁾

lidity of the obtained results, we have also performed the plaquette expansion starting from another initial configuration, where an isolated plaquette is formed by four spins shown as 1, 2, 3 and 4 in Fig. 1(a). From the ground state energy computed up to the seventh order, we confirm that the phase boundaries obtained by two distinct ways are indeed consistent within our accuracy.

To complete our discussions on this model, it is necessary to discuss whether the system is driven to the magnetically ordered phase with the increase of the interchain coupling. To this end, we calculate the staggered susceptibility χ_{AF} and the spin gap Δ by means of the plaquette expansion up to the fourth and the fifth order in λ , respectively. We show the results obtained for $k = 0.9$ and 0.8 in Fig. 4. It is seen that two lines determined from different quantities provide consistent values even around $\lambda = 1$, implying that the phase boundary may be obtained rather accurately for the original model ($\lambda = 1$) although our calculation is restricted to the lower-order series expansion. From the above analyses, we end up with the phase boundary shown in Fig. 3, which separates the plaquette phase II and the magnetically ordered phase III. Note that for large α , the boundary between II and III approaches the correct asymptotic line, which was estimated as $k_c = 0.56$.²⁰⁾ This also supports that the present calculation gives the reliable results for the phase diagram.

In the obtained phase diagram shown in Fig. 3, we remark again that two competing spin-gap states in the orthogonal dimer chain^{11,18)} are continuously connected to those in Shastry-Sutherland model. In particular, a RVB-like intermediate spin-gap phase⁶⁾ proposed for the Shastry-Sutherland model naturally emerges via the adiabatic continuation of the plaquette phase in the

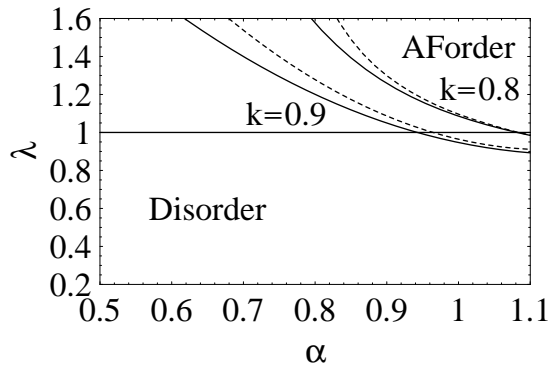


Fig. 4. Second-order phase transition between the plaquette phase and the antiferromagnetically ordered phase for the 2D spin system given by Fig. 1(a) (for $k = 0.9$ and 0.8). The solid (dashed) line indicates the phase boundary obtained by biased $[3/2]$ ($[2/2]$) Padé approximants for the spin gap (the staggered susceptibility).

orthogonal-dimer chain.

4.2 Adiabatic evolution from the 1/5-depleted square lattice

We next deal with the spin system with a slightly different structure shown in Fig. 1(b). Recall that when $k = 1$ ($k = 0$), this model with $\lambda = 1$ is reduced to the Shastry-Sutherland model (1/5-depleted square lattice model). We here study how the spin-gap phase in the orthogonal-dimer model for $\text{SrCu}_2(\text{BO}_3)_2$ is related to that in the 1/5-depleted square-lattice model for CaV_4O_9 , when the frustrating interaction k is continuously varied. We carry out the dimer (plaquette) expansion for the ground-state energy, the staggered susceptibility and the spin gap. By performing similar asymptotic analyses mentioned above, the phase diagram is determined, which is shown in Fig. 5. The detail of calculation will be described below for each case.

Let us start our discussions with the case of $k = 0$, i.e. the 1/5-depleted square lattice model, which was already studied in connection with CaV_4O_9 .¹²⁾ In this case, as the ratio of the exchange interactions α is changed, the dimer phase I first undergoes the second-order phase transition to the antiferromagnetically ordered phase IV at the critical point $\alpha_{c2}^l = 0.590(5)$, and this ordered phase further shows the second-order phase transition to the plaquette phase II at $\alpha_{c2}^u = 1.09(1)$. The critical points obtained by the present method agree fairly well with those of quantum Monte Carlo simulations.¹²⁾ Note that the antiferromagnetically ordered phase on 1/5-depleted square lattice labeled by IV is different from that on the square lattice indicated by III.

As the coupling k is increased, the spin-gap phases become more stable while the magnetic correlation for the phase IV is suppressed, which is mainly due to the frustrating nature of the interaction k . It is seen that the competition among three phases persists up to the multicritical point $(\alpha, k\alpha) \simeq (0.72, 0.32)$ beyond which the magnetically ordered phase IV disappears. Thus for

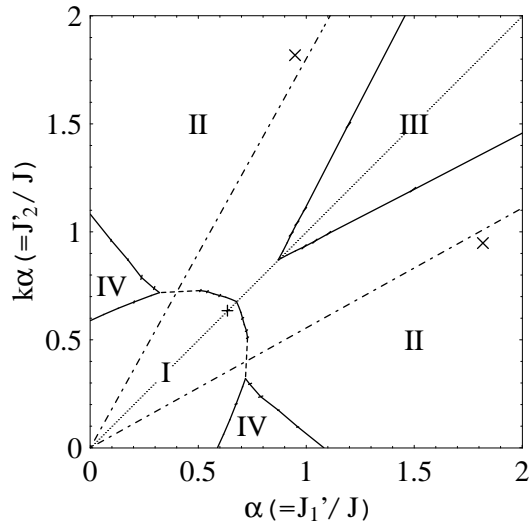


Fig. 5. Phase diagram for the 2D frustrated spin system shown in Fig. 1(b). The phase I and II represent the dimer and the plaquette phase. The phase III (IV) represents the antiferromagnetically ordered phase on the square lattice (1/5-depleted square lattice). The dotted line indicates the 2D Shastry-Sutherland model and the dot-dashed lines the asymptotic phase boundary for large α . The crosses + and × indicate the location of $\text{SrCu}_2(\text{BO}_3)_2$ ¹⁹⁾ and CaV_4O_9 ,⁹⁾ respectively.

larger k the dimer state directly undergoes the first-order phase transition to the plaquette spin-gap phase. Note that the dimer phase here does not have the exact eigenstate except for the orthogonal-dimer case $k = 1$, which is contrasted to the model (a). We thus have estimated the ground state energy both of the dimer and the plaquette phases in this case. For reference, we show in Fig. 6 the ground-state energy calculated for $k = 0.9$, where the dimer (plaquette) expansion has been first performed up to the eighth (seventh) order in λ , and then the first-order inhomogeneous differential method has been used to obtain the values at $\lambda = 1$. To confirm the valid-

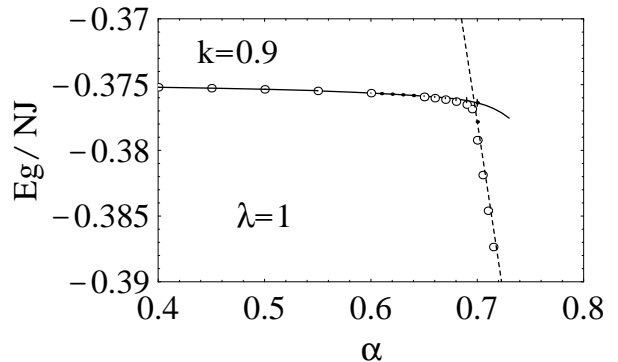


Fig. 6. Ground state energy per site as a function of $\alpha = J'_1/J$ (for $\lambda = 1$ and $k = 0.9$) for the model shown in Fig. 1(b). The solid (dashed) line indicates the energy for the dimer (plaquette) phase. We also show the results obtained by the exact diagonalization for $N = 24$ sites with a periodic boundary condition as open circles.

ity of our series expansion, we have also performed the

exact diagonalization for the system with $N = 24$ sites with a periodic boundary condition, which is found to be consistent with the series-expansion results. The phase boundary thus obtained between two spin-gap phases is drawn in Fig. 5. We note that our series expansion turns out to be not so accurate around the tricritical point, so that the phase boundary around there is shown as the dashed line.

When the coupling k is further increased, the plaquette phase shows the instability to an antiferromagnetically ordered phase III on the square lattice. To study this instability from II to III, we have performed the plaquette expansion for the staggered susceptibility (spin gap) up to the fourth (fifth) order, and determined the phase boundary using the biased Padé approximants, which is shown in Fig. 5.

Consequently, we arrive at the phase diagram shown in Fig. 5, in which the parameters deduced for the spin-gap compounds CaV_4O_9 and $\text{SrCu}_2(\text{BO}_3)_2$ are also indicated. It is clearly seen how the 2D Heisenberg model on the $1/5$ -depleted square lattice is connected to the Shastry-Sutherland model. It is particularly interesting to notice that a RVB-type spin gap state proposed for the Shastry-Sutherland model is adiabatically connected to a plaquette singlet state for CaV_4O_9 .

4.3 Excitation spectrum

We have seen that the spin-gap phases in the Shastry-Sutherland model are continuously connected to the spin-gap phases known for two different models. According to this relationship, it may be expected that the Shastry-Sutherland model shares some of its characteristic features with the latter models. As an example, we here show that the spin-triplet excitation spectrum for the RVB-type phase in the Shastry-Sutherland model indeed exhibits a similar behavior expected for the plaquette phase in the orthogonal-dimer chain. In Fig. 7(a), we show the spin-triplet excitation spectrum calculated for the 2D Shastry-Sutherland model. In contrast to the dimer phase, where the lowest triplet excitation is an almost-localized triplet over the dimer ground state,⁴⁾ we find that the lowest-triplet excitation in the RVB-type phase shows a more complicated feature; two triplet excitations show the level-crossing around value of $\alpha' \simeq 0.76$. It is not easy to clearly see the origin of this level-crossing because our calculation for the 2D model is restricted to lower-order perturbation. Fortunately, we can exploit the idea of the adiabatic continuation by continuously changing the system to the orthogonal-dimer chain.

In the orthogonal-dimer chain, a similar level-crossing was recently observed,¹¹⁾ as shown in Fig. 7(b). In this case, the nature of two different excitations in the plaquette phase is well understood. Namely, in the lowest excitation denoted by the dotted line in the region of $\alpha > \alpha' (\simeq 0.87)$ is a triplet excitation that simply breaks a plaquette singlet. On the other hand in the region $\alpha_{c1} < \alpha < \alpha'$, the lowest-energy excited state shown by the dashed line is described by a four-fold degenerate level without dispersion,¹¹⁾ in which two diagonal spins on a square plaquette becomes completely free, giving rise to the four-fold degeneracy.¹¹⁾ The emergence of this

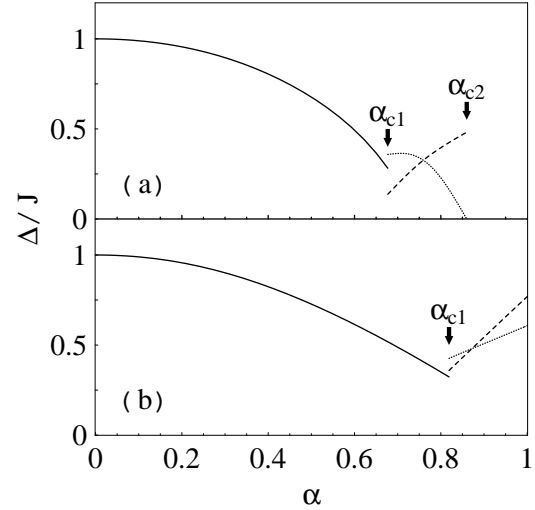


Fig. 7. Spin-triplet excitation energy Δ/J for (a) Shastry-Sutherland model and (b) orthogonal-dimer chain as a function of $\alpha (= J'_1/J)$. In (a), a triplet excitation spectrum¹⁴⁾ over the dimer state is plotted for $\alpha < \alpha_{c1}$, while two lowest triplet excitations are shown for the RVB-type phase $\alpha_{c1} < \alpha < \alpha_{c2}$. In (b), similar plot is done for the dimer phase ($\alpha < \alpha_c$) and also for the plaquette phase ($\alpha_c < \alpha$).¹¹⁾ The meaning of the solid, dashed and dotted lines is mentioned in the text.

peculiar excitation reflects the fact that the system is located closely to the first-order phase transition point. In other words, this level crossing is due to the strong frustration effect around the transition point. When the interchain coupling k is introduced, the above two-types of excitations are continuously changed to those in the Shastry-Sutherland model, as shown in Fig. 7(a). In particular, four-fold degenerate states in the chain system split into singlet and triplet states, and the latter gives the lowest-excited state shown by the dashed line in the Shastry-Sutherland model in Fig. 7(a). In this way, the characteristic level-crossing found in the 1D system persists even for the 2D system, from which we can say that the unusual level-crossing found in the Shastry-Sutherland model reflects the strong frustration around the first-order phase transition point.

§5. Summary

We have studied the ground-state phase diagram for a frustrated quantum spin model on the square lattice, which systematically describes the systems for the spin-gap compounds such as $\text{SrCu}_2(\text{BO}_3)_2$ and CaV_4O_9 . By calculating the ground state energy, the staggered susceptibility and the spin gap by means of the series expansion method, we have determined the phase diagram, and clarified the nature of the associated quantum phase transitions. One of the main purpose of the present study is to uncover the origin of the intermediate spin-gap state proposed for the Shastry-Sutherland model, which has a spatially extended nature. Starting from two types of the well-studied models, we have observed how this intermediate phase emerges in the phase diagram. Namely, with the use of the simple orthogonal-dimer chain model, it has been checked that the first-order phase transition

between the dimer and RVB-type phases in the Shastry-Sutherland model has the same origin as in the transition between the dimer and plaquette phases known for the chain system. Further analysis based on the second model has allowed us to show that the RVB-type intermediate state is adiabatically connected to the plaquette state known for the $1/5$ -depleted square lattice model, which describes the essential properties of CaV_4O_9 . We have also shown that the level-crossing of the triplet excitations in the Shastry-Sutherland model is understood well in terms of their counterparts in the 1D orthogonal-dimer chain model.

These systematic investigations based on the adiabatic continuation support that the intermediate spin-gap phase for the Shastry-Sutherland model may be stabilized by geometrical frustration induced by the competing interactions. However, we wish to mention that there still remain unresolved problems for the phase diagram of the Shastry-Sutherland model. For example, Weihong *et al.* have shown by means of the Ising expansion¹⁴⁾ that the system has the finite staggered magnetization down to $(J'/J) \simeq 0.71$, which may contradict the fact that the spin gap phase is extended up to $(J'/J) \simeq 0.86$. Although we have checked that the ground state energy of the present spin-gap phase for $(J'/J) < 0.86$ is indeed lower than that of Weihong *et al.*, this apparent inconsistency for the magnetization should be resolved in the future study. Also, Knetter *et al.* have recently claimed that the instability of the two-magnon excitation in the dimer phase may occur at $(J'/J) = 0.630(5)$.⁷⁾ Although it may not be clear whether this indeed triggers a first-order phase transition to some new phase,⁷⁾ it is an important open problem to answer the above points for the phase diagram of the Shastry-Sutherland model. This is now under consideration.

The work is partly supported by a Grant-in-Aid from the Ministry of Education, Science, Sports, and Culture. A.K. is supported by the Japan Society for the Promotion of Science.

- 1) H. Kageyama, K. Yoshimura, R. Stern, N. V. Mushnikov, K. Onizuka, M. Kato, K. Kosuge, C. P. Slichter, T. Goto and Y. Ueda, Phys. Rev. Lett. **82** (1999) 3168.
- 2) S. Taniguchi, Y. Nishikawa, Y. Yasui, Y. Kobayashi, M. Sato, T. Nishioka, M. Kontani and K. Sano, J. Phys. Soc. Jpn. **64** (1995) 2758.
- 3) B. S. Shastry and B. Sutherland, Physica **108B** (1981) 1069.
- 4) S. Miyahara and K. Ueda, Phys. Rev. Lett. **82** (1999) 3701.
- 5) M. Albrecht and F. Mila, Europhys. Lett. **34** (1996) 145.
- 6) A. Koga, and N. Kawakami, Phys. Rev. Lett. **84** (2000) 4461.
- 7) C. Knetter, A. Bühler, E. M.-Hartmann and G. S. Uhrig, Phys. Rev. Lett. **85** (2000) 3958.
- 8) K. Ueda, H. Kontani, M. Sigrist and P. A. Lee, Phys. Rev. Lett. **76** (1996) 1932; N. Katoh and M. Imada, J. Phys. Soc. Jpn. **64** (1995) 4105.
- 9) Y. Fukumoto and A. Oguchi, J. Phys. Soc. Jpn. **67** (1998) 2205.
- 10) Z. Weihong, J. Oitmaa and C. J. Hamer, Phys. Rev. B **58** (1998) 14147.
- 11) A. Koga, K. Okunishi and N. Kawakami, Phys. Rev. B **62** (2000) 5558.
- 12) M. Troyer, H. Kontani and K. Ueda, Phys. Rev. Lett. **76** (1996) 3822.
- 13) R. R. P. Singh, M. P. Gelfand and D. A. Huse, Phys. Rev. Lett. **61** (1988) 2484.
- 14) Z. Weihong, C. J. Hamer and J. Oitmaa, Phys. Rev. B **60** (1999) 6608.
- 15) A. J. Guttmann, in *Phase Transitions and Critical Phenomena*, edited by C. Domb and J. L. Lebowitz (Academic, New York, 1989) Vol. 13.
- 16) S. Chakravarty, B. I. Halperin and D. R. Nelson, Phys. Rev. Lett. **60** (1988) 1057; Phys. Rev. B **39** (1989) 2344.
- 17) M. Ferer and A. Hamid-Aidinejad, Phys. Rev. B **34** (1986) 6481.
- 18) N. B. Ivanov and J. Richter, Phys. Lett. **232A** (1997) 308; J. Richter, N. B. Ivanov and J. Schulenburg, J. Phys. Condensed Matter **10** (1998) 3635.
- 19) S. Miyahara and K. Ueda, J. Phys. Soc. Jpn. Suppl. B **69** (2000) 72.
- 20) Y. Fukumoto and A. Oguchi, J. Phys. Soc. Jpn. **67** (1998) 697; J. Phys. Soc. Jpn. **67** (1998) 2205; Z. Weihong, J. Oitmaa and C. J. Hamer, Phys. Rev. B **58** (1998) 14147; R. R. P. Singh, Z. Weihong, C. J. Hamer and J. Oitmaa, Phys. Rev. B **60** (1999) 7278; A. Koga, S. Kumada and N. Kawakami, J. Phys. Soc. Jpn. **68** (1999) 2373; **69** (2000) 1843.